
Article:
Mansfeld, J., Collin, P., Collins, M.O. orcid.org/0000-0002-7656-4975 et al. (2 more authors) (2011) APC15 drives the turnover of MCC-CDC20 to make the spindle assembly checkpoint responsive to kinetochore attachment. NATURE CELL BIOLOGY, 13 (10). pp. 1234-1243. ISSN 1465-7392

https://doi.org/10.1038/ncb2347

Nat Cell Biol. Author manuscript; available in PMC 2012 April 01.

Published in final edited form as:
Nat Cell Biol. ; 13(10): 1234–1243. doi:10.1038/ncb2347.

APC15 drives the turnover of MCC-Cdc20 to make the Spindle Assembly Checkpoint responsive to kinetochore attachment

Jörg Mansfeld[1], **Philippe Collin**[1,3], **Mark O. Collins**[2,3], **Jyoti S. Choudhary**[2], and **Jonathon Pines**[1]

[1]The Gurdon Institute and Department of Zoology, Tennis Court Road, Cambridge CB2 1QN

[2]Proteomic Mass Spectrometry Laboratory, The Wellcome Trust Sanger Institute, Cambridge, UK

Abstract

Faithful chromosome segregation during mitosis depends on the Spindle Assembly Checkpoint (SAC) that monitors kinetochore attachment to the mitotic spindle. Unattached kinetochores generate mitotic checkpoint proteins complexes (MCCs) that bind and inhibit the Anaphase Promoting Complex/Cyclosome (APC/C). How the SAC proficiently inhibits the APC/C but still allows its rapid activation when the last kinetochore attaches to the spindle is important to understand how cells maintain genomic stability. We show that the APC/C subunit APC15 is required for the turnover of the APC/C co-activator Cdc20 and release of MCCs during SAC signalling but not for APC/C activity per se. In the absence of APC15, MCCs and ubiquitylated Cdc20 remain 'locked' onto the APC/C, which prevents the ubiquitylation and degradation of Cyclin B1 when the SAC is satisfied. We conclude that APC15 mediates the constant turnover of Cdc20 and MCCs on the APC/C to allow the SAC to respond to the attachment state of kinetochores.

Introduction

To maintain genomic stability each daughter cell must receive an identical set of sister chromosomes at mitosis. This is ensured by the SAC, which surveys the attachment state of kinetochores and prevents the APC/C targeting Cyclin B1 and securin for degradation until the last kinetochore attaches to the spindle. The APC/C is inactive because its co-activator Cdc20 is sequestered into MCCs that are initially composed of the Mad2, BubR1 and Bub3 checkpoint proteins [1] that accumulate at unattached kinetochores. How Cdc20 is incorporated into the MCC and how it is released from the APC/C and MCCs after the SAC has been satisfied is currently debated.

Contradictory mechanisms have been proposed to release Cdc20 and inactivate MCCs, including APC/C-dependent proteolysis [2, 3], or the polyubiquitylation but not degradation of Cdc20 to release Mad2 and the MCC from the APC/C [4]. Both mechanisms have been questioned because a non-ubiquitylatable mutant of Cdc20 dissociates from checkpoint proteins when the SAC is inactivated and overrides the SAC [5].

Correspondence to JP: jp103@cam.ac.uk.
[3]These authors contributed equally

Author contributions JM performed all the experiments, PC generated the RPE1-Cyclin A2- and B1-Venus knock-in cell lines, MOC and JC performed the mass spectrometry that identified APC15 and the Cdc20 ubiquitylation site. JM and JP designed the experiments and wrote the paper. All the authors contributed to the interpretation of the results.

Europe PMC Funders Author Manuscripts

Here, we identify the protein C11orf51 (hereafter referred to as APC15) as a subunit of the human APC/C required for the release of MCCs from the APC/C and the degradation of Cdc20. Depleting APC15 increases the amount of Cdc20 and MCCs on the APC/C, which persist after the SAC is satisfied, thereby delaying progress through mitosis. APC15 depletion, however, does not affect APC/C activity when MCC formation is prevented. We show that the dissociation of MCCs, and in particular Mad2, proceeds independently of Cdc20 ubiquitylation; indeed ubiquitylated Cdc20 and Mad2 both accumulate on the APC/C in the absence of APC15. Nonetheless, APC11 also contributes to the dissociation of MCCs, indicating that the ubiquitylation of a protein(s) other than Cdc20 may be required. Our data provide new insights into how the SAC is made responsive to microtubule attachment.

Results

APC15 is a subunit of the human APC/C

We identified C11orf51 in a systematic proteomic analysis of the APC/C purified from HeLa cell extracts. Human C11orf51 is conserved in animals and has sequence similarity to the *Schizosaccharomyces pombe* APC/C subunit Apc15 [6] and *Saccharomyces cerevisiae* Mnd2 [7]; therefore, we named it APC15 (Supplementary Fig. S1a online).

To characterise APC15, we used recombinant human APC15 to raise a polyclonal antibody that recognised a protein of the predicted molecular mass (14.3 kDa) on immunoblots from HeLa cell extracts whose abundance was reduced after siRNA treatment with APC15-specific oligonucleotides, and co-migrated with recombinant APC15 (Supplementary Fig. S1b online). All the detectable APC15 co-precipitated with other APC/C subunits (Fig. 1a) throughout the cell cycle (Fig. 1b), and co-migrated with them in size-exclusion chromatography (Fig. 1c). APC15 required APC8 for stability and to be incorporated into the APC/C (Fig. 1d; Supplementary Fig. S2a, b online), and *in vitro* binding assays and the recent structure of *S. cerevisiae* APC/C indicated that Mnd2 also associated with Apc8 [7, 8]. Moreover, *MND2Δ* and *CDC23-1* (APC8) mutants are synthetically lethal [9] and human APC15 was detected in APC8-GFP immunoprecipitates [10].

APC15 depletion delays anaphase and Cyclin B1 degradation

To elucidate the function of APC15 we used five different siRNAs that reduced the abundance of APC15 in HeLa and in hTert-immortalised human retinal pigment epithelial (RPE1) cells (Fig. 2a). We analysed the effect of depleting APC15 on progress through mitosis in RPE1 cell lines in which the Venus fluorescent protein had been ‘knocked-in’ to one allele of the Cyclin B1 or Cyclin A2 gene (PC, O. Naschekina, and J.P, in preparation); therefore, the intensity of the Venus fluorescence was directly correlated with the abundance of endogenous Cyclin A2 and B1. Depleting APC15 by any of the siRNA treatments delayed progress from nuclear envelope breakdown (NEBD) to anaphase in cycling cells by at least a factor of two (Fig. 2b: 22 ± 3 min in control cells; 44 ± 21 to 54 ± 28 min in APC15-depleted cells, see Supplementary Information Table 1 online for statistical analyses). This phenotype was caused by the lack of APC15 because siRNA-resistant APC15 eliminated the delay (Supplementary Fig. S3c online). In APC15-depleted cells chromosomes aligned at the same time as in controls, but cells subsequently arrested with a well-formed metaphase plate (Fig. 2c).

Assaying Cyclin B1-Venus fluorescence in single cells [11] revealed that APC15-depleted cells initiated Cyclin B1 degradation slightly later and degraded it at a slower rate than did controls (Fig. 2d; Supplementary Fig. S3a, b online), whereas inactivating the APC/C by depleting APC3 stabilised Cyclin B1 and severely delayed mitosis (Figs 2d, 3b) [12, 13]. By contrast, depleting APC15 did not appear to affect APC/C activity because the kinetics of

Cyclin A2 degradation, a SAC-independent substrate [14], was largely unchanged, although degradation was slower shortly before anaphase compared to control cells. The time of this divergence correlated with the satisfaction of the SAC (marked by an asterisk Fig. 2e), and maintaining the SAC with dimethylenastron (DMA) also slowed Cyclin A2-Venus degradation (Fig. 2e). The slow down in Cyclin A2-Venus degradation in APC15-depleted cells was explained by the prolonged presence of MCCs on the APC/C (see below), which competed with Cyclin A2 for Cdc20 [14].

In agreement with single cell analyses, immunoblots of APC15-depleted HeLa cells progressing through mitosis showed a delay in Cyclin B1 but not Cyclin A2 degradation, and also revealed that Cdc20 was stabilised (Supplementary Fig. S2c online).

APC15 functions through the SAC but is not required for APC/C activity

Cdc20 is degraded when the SAC is active [5, 15-17], therefore, the stabilisation of Cdc20 and Cyclin B1, but not Cyclin A2, indicated that depleting APC15 probably perturbed the regulation of the APC/C by the SAC. To test this, we assayed APC/C activity in APC15-depleted cells after abrogating the SAC either by co-depleting Mad2 [18, 19], or treating cells with 0.5 μM reversine, an inhibitor of the Mps1 kinase [20]. Both treatments eliminated the metaphase delay (Fig. 3a, b). This indicated that in the absence of the SAC, APC/C activity was likely to be the same in control and APC15-depleted cells. We confirmed this by treating control and APC15-depleted cells with reversine, which showed that Cyclin B1 was degraded with very similar rates in control and APC15-depleted cells (Fig. 3c), and that the kinetics of Cyclin A2 degradation in control, DMA-treated, and APC15-depleted cells were identical (Fig. 3d).

To support our conclusion that depleting APC15 did not directly affect APC/C activity, we sensitised the APC/C by co-depleting APC15 and another APC/C subunit, APC10. Apc10 deletions in *S. cerevisiae* are viable but APC/C purified from these cells was less processive in ubiquitylating the B-type cyclin, Clb2 [21]. To assay APC/C activity independently of the SAC we used reversine and observed that, as predicted, the depletion of APC10 slightly reduced the rate of Cyclin B1-Venus degradation, but co-depleting APC15 and APC10 did not have an additive effect (Supplementary Information Fig. S4a online).

To verify that APC15 did not contribute to APC/C activity in the absence of the SAC, we assayed interphase APC/C activity *in vitro* using purified components 22. Control- and APC15-depleted APC/C showed almost identical activity against Cyclin B1 (Fig. 3e).

We conclude that depleting APC15 does not affect APC/C activity *per se* but causes a SAC-dependent delay in both the destruction of Cyclin B1 and the initiation of anaphase.

APC15 depletion increases the association between the APC/C and the MCC

To determine how APC15 influenced APC/C activity through the SAC we analysed APC/C and SAC complexes in cells depleted of APC15. As a positive control we compared them to complexes from p31^{comet}–depleted cells. p31^{comet} antagonises the dimerisation of the two conformations of Mad2 and is required to inactivate the SAC [23-27]. In cells treated with DMA to impose the SAC, depleting APC15 stabilised Cdc20 and caused a three to four fold increase in the amounts of Mad2 and Bub3, and a two-fold increase in BubR1 and Cdc20, bound to the APC/C (Fig.4a, Supplementary Information Table 1 online). All these effects were rescued by expressing a siRNA-resistant APC15 (Supplementary Fig. S4b online). Depleting p31^{comet} had a smaller effect and influenced mainly the amount of Mad2 precipitating with the APC/C (Fig. 4a). We also analysed Cdc20 immunoprecipitates from the same extracts to determine the effect on MCCs that were not bound to the APC/C and found that depleting APC15 or p31^{comet} caused a two to three fold increase in Mad2 and

Bub3 levels co-precipitating with Cdc20 (Fig. 4b). Size-exclusion chromatography confirmed that depleting APC15 enriched Mad2 on the APC/C, and enriched both Cdc20 and Mad2 in APC/C-unbound MCCs (control: $Cdc20^{APC/C}$ vs. $Cdc20^{MCC}$ = 2:1; APC15 siRNA: $Cdc20^{APC/C}$ vs. $Cdc20^{MCC}$ = 1.25:1). Consequently, the pool of free Mad2 decreased from 88% in control to 50% in APC15-depleted cells (Fig. 4c, Supplementary Fig. S5a, b online). Depleting $p31^{comet}$ only increased the amount of Cdc20 and Mad2 in unbound MCCs ($Cdc20^{APC/C}$ vs. $Cdc20^{MCC}$ = 1:1.75, Fig. 4c, Supplementary Fig. S5c online).

These experiments indicated that during SAC signalling there was a flux of MCC-Cdc20 on and off the APC/C that was blocked in the absence of APC15, and that $p31^{comet}$ was required for the turnover of non-APC/C-bound MCCs. If so, one consequence might be that during the SAC a population of APC/C could briefly be devoid of MCCs (apo-APC/C [28]) and able to bind free Cdc20 and degrade some Cyclin B1. This could be one explanation for why some cancer cells 'slip' out of mitosis as a consequence of the slow proteolysis of Cyclin B1 [29-31]. Interfering with APC15 or $p31^{comet}$, which should reduce the population of apo-APC/C, provided some support for this model because it markedly reduced mitotic slippage in the presence of 5 μM taxol (Supplementary Fig. S4c online: $t_{50\%\ slippage}$ in control cells 258 min, in si-APC15 cells 1094 min, in si-$p31^{comet}$ cells 624 min).

APC15 is required for the release from SAC inhibition

To determine what happens when SAC signalling is turned off we treated cells with the Aurora B inhibitor ZM447439 [32], which inactivates or satisfies the SAC [33]. Compared to control-depleted cells, ZM447439 treatment did not reduce the NEBD to anaphase delay in APC15-depleted cells (Fig. 5a; Supplementary Information Table 1 online). This indicated that in the absence of APC15, MCCs might not be released from the APC/C after the SAC had been satisfied.

To test the requirement for APC15 to dissociate MCCs from the APC/C we released cells from a DMA-block into fresh medium containing MG132 (to block mitotic exit) and monitored the dissociation of SAC proteins from the APC/C over time. Whereas MCCs readily dissociated from the APC/C in control cells, both APC15-and $p31^{comet}$-depletion stabilised BubR1, Mad2 and Bub3 on the APC/C (Supplementary Fig. S6a online).

To measure the dissociation of MCC components from the APC/C independently of the variable time required for kinetochores to attach to microtubules and satisfy the SAC, we repeated the experiment in the presence of reversine to inactivate the SAC. Again, depleting APC15 strongly impaired the release of MCCs, whereas $p31^{comet}$-depletion showed a less pronounced effect (Fig 5b, Supplementary Fig. S6b online), indicating that APC15 and $p31^{comet}$ might regulate different aspects of the SAC. Indeed, depleting both APC15 and $p31^{comet}$ had an additive effect on the delay from NEBD to anaphase (97±25 min, Supplementary Fig. S7a online). Importantly, APC15 depletion did not affect the transient interaction of $p31^{comet}$ with the APC/C, excluding the possibility that $p31^{comet}$ acts through APC15 to release MCCs from the APC/C (Supplementary Fig. S7b, c online).

MCC components had been shown to dissociate from the APC/C purified from SAC-arrested cells during *in vitro* ubiquitylation reactions [4] concomitantly with an increase in Cyclin B1 ubiquitylation (Supplementary Fig. S6c, d online). We confirmed this result and found that this release also required APC15 because, compared to control-depleted cells, APC/C purified from APC15-depleted cells retained MCCs and these inhibited the ubiquitylation of Cyclin B1 (Fig. 5c, d; Supplementary Fig. S6e, f online). Since *in vitro* ubiquitylation reactions do not contain the components that generate a SAC signal (kinetochores), we conclude that the role of APC15 in the release of the MCC is constitutive

and intrinsic to the APC/C. However, we cannot exclude that *in vivo* upon satisfaction of the SAC there is crosstalk between the SAC and the APC/C that might involve APC15.

To provide further evidence that APC15 reduces APC/C activity by retaining MCCs on the APC/C, and not because APC15 directly contributes to APC/C activity, we purified mitotic APC/C from control and APC15-depeleted cells that was devoid of MCCs. We synchronised HeLa cells and added MG132 and reversine shortly before NEBD. APC/C immunoprecipitates from control and APC15-depleted cells had no detectable Bub3, almost no Mad2 and only marginal amounts of BubR1, even though APC15 was efficiently depleted (Supplementary Fig. S7d online). *In vitro* ubiquitylation reactions showed that the mitotic APC/C was equally as active when purified from control- or from APC15-depleted cells. By contrast, APC/C from APC11-depleted cells was markedly less active (Supplementary Fig. S7e online). We conclude that APC15 is not required for APC/C activity in mitosis.

Cdc20 ubiquitylation is not required to dissociate MCCs from the APC/C

The ubiquitylation of Cdc20 has been proposed to disassemble MCCs by interfering with Mad2-binding through eliciting a conformational change in Cdc20, or by direct steric occlusion of the Mad2 binding surface [4]. Since APC15 depletion stabilised Cdc20 (Figs 4a, 7a, Supplementary Fig. S2c online,) we analysed whether APC15-depletion prevented Cdc20 ubiquitylation, which might also explain the elevated amount of Mad2 on the APC/C. In contrast, we found that in the absence of APC15 both ubiquitylated Cdc20 and Mad2 were enriched on the APC/C (Fig. 6a, b), indicating that the ubiquitylation of Cdc20 did not disrupt the MCC. This agreed with our previous observation that a non-ubiquitylatable Cdc20 mutant (in which all the lysines were mutated to arginine) could be released from APC/C-unbound MCCs when the SAC was satisfied [5]. Nevertheless, the mechanism of Cdc20-release might differ between APC/C-bound and –unbound MCCs [34, 35]; therefore, we sought to determine whether a non-ubiquitylatable Cdc20 could be released from APC/C-bound complexes.

Our mass spectrometry analysis of the APC/C had identified lysine 490, close to the carboxyl-terminus of Cdc20, as ubiquitylated in prometaphase (Supplementary Fig. S8a online), in agreement with a recent mass spectrometry study, which reported that the neighbouring lysine 485 could also be ubiquitylated [36]. Mutating just these two lysines to arginine completely prevented ubiquitylation and had no effect on the ability of Cdc20 to bind the APC/C (Fig. 6c, d). Moreover, $Cdc20^{K485/490R}$ dissociated with the other MCC components from the APC/C with comparable efficiency to wild type Cdc20 ($Cdc20^{WT}$, Fig 6c, e). Therefore, we conclude that Cdc20 ubiquitylation is not required to dissociate Mad2 and the MCC from the APC/C.

APC11 contributes to the release of MCCs from the APC/C

To test whether the increase of MCCs on the APC/C is specific to APC15 depletion, we monitored MCC binding to the APC/C during SAC signalling in the absence of several other APC/C subunits. Depleting APC3 had no effect, whereas depleting APC6 and APC8 strongly reduced MCC binding to the APC/C (Supplementary Fig. S8b online). This result was expected because we recently showed that APC8 was required to recruit MCC-Cdc20 to the APC/C [13], and APC8 required APC6 to incorporate into the APC/C (Fig. 1d). To reduce APC/C activity directly we depleted APC10, which should primarily affect activity in metaphase [13] and APC11, which should inactivate the APC/C entirely [37, 38]. Depleting APC11, but not APC10, stabilised Cdc20 and Cyclin A during SAC signalling (Fig. 7a). Depleting APC11 also increased the amount of MCCs on the APC/C when the SAC was imposed by DMA, though to a lesser extent than APC15 depletion (Fig. 7b, c). When cells were released from this arrest into fresh medium containing reversine and MG132 fewer

MCCs dissociated from the APC/C in the absence of APC11 compared to control APC/C (Fig. 7d, Supplementary Fig. S8c online).

To confirm that APC/C ubiquitylation activity was required for the release of MCCs we depleted UbcH10, an E2 specifically used by the APC/C [22, 39]. Depleting UbcH10 enriched Mad2 and Bub3 on the APC/C to a similar extent as depleting APC11 but had no effect on the dissociation of MCCs (Fig. 7c, e; Supplementary Fig. S8e online), As a result, by the end of the time course the APC/C from UbcH10-depleted cells contained only slightly elevated amounts of BubR1, Mad2 and Bub3 compared to control cells (Fig. 7e; Supplementary Fig. S8d online). This was in agreement with our observation that depleting UbcH10 *in vivo* had little or no effect on mitosis in cycling cells [40]. Thus, although Cdc20 ubiquitylation was irrelevant to the release of MCCs, the effect of depleting APC11 and UbcH10 indicated that other proteins might have to be ubiquitylated for MCC turnover on the APC/C.

Discussion

We have identified an APC/C subunit that is primarily required for the turnover of checkpoint complexes on the APC/C and thus the responsiveness of the SAC. The turnover of MCCs on the APC/C during SAC signalling continuously generates APC/C devoid of MCCs and Cdc20 (apoAPC/C [28]) that would be available for the rapid activation of the APC/C when the SAC is satisfied. In the absence of APC15 the MCC remains 'locked' onto the APC/C with ubiquitylated Cdc20, causing MCCs that are not yet bound to the APC/C to accumulate. Our evidence indicates that p31^{comet} has an important role in the turnover of these unbound MCCs (Supplementary Fig. S9a, b online).

That the phenotype of APC15-depletion depends on SAC signalling might indicate that depleting APC15 itself imposes the SAC, or that APC/C activity is compromised and countered by abrogating the SAC. However, several lines of evidence argue against these possibilities. It is unlikely that APC15 depletion activates the SAC, because inactivating the SAC after MCCs have been recruited to the APC/C has no effect on the APC15-dependent delay in mitosis: only abrogating the SAC before mitosis rescues APC15 depletion. Several lines of evidence show that depleting APC15 does not compromise APC/C activity: i) the degradation of Cyclin A is hardly affected in the absence of APC15; ii) the kinetics of Cyclin B1 destruction is identical to controls in the absence of the SAC; iii) APC15 is not required for APC/C activity *in vitro*; iv) Cdc20 ubiquitylation is not affected by APC15 depletion although Cdc20 itself is stabilised, possibly because it cannot be released from the APC/C to be degraded by the proteasome. By contrast, directly inactivating the APC/C by depleting APC11 stabilises both Cdc20 and Cyclin A. We note that APC15 deletions in *S. pombe* or in *S. cerevisiae* [6, 7] also show that APC15 is not required for APC/C activity.

How APC15 promotes the release of Mad2 and Bub3 from the APC/C is not clear, but we can conclude that Cdc20 ubiquitylation is not required because we find ubiquitylated Cdc20 on the APC/C in the absence of APC15; indeed, both Mad2 and ubiquitylated Cdc20 simultaneously accumulate on the APC/C. Furthermore, replacing endogenous Cdc20 with a non-ubiquitylatable mutant does not affect the release of MCCs from the APC/C. Instead, as we previously suggested, the ubiquitylation of Cdc20 may be important to target Cdc20 for proteolysis to maintain the SAC and prevent that increasing amounts of Cdc20 could eventually overcome the SAC [5, 16]. The alternative model, that Cdc20 ubiquitylation drives the disassembly of the MCC, raises some conceptual problems: the constant generation of ubiquitylated Cdc20, which would be insensitive to the SAC [4] might immediately activate the APC/C. To resolve this, Cdc20 has been reported to be deubiquitylated by USP44 [41], but this would generate a futile cycle because this Cdc20 would now be able to activate the APC/C.

Our data indicate that a factor other than Cdc20 might need to be ubiquitylated since depleting UbcH10 increases the amounts of Mad2 and Bub3 on the APC/C during SAC signalling and APC11 depletion prevents the release of MCCs from the APC/C. BubR1 is one attractive candidate because we previously showed that it can be ubiquitylated by the APC/C *in vitro* [22], which might be important for progress through mitosis [42]. Nonetheless, although polyubiquitylation appears to be required to release MCCs [4, 34], proteolysis is not [4, 5, 28, 34].

In contrast to APC11, inactivating the APC/C by depleting APC3 does not increase the amounts of MCCs on the APC/C, and depleting APC10 slightly decreases MCCs on the APC/C. This may indicate that APC3 contributes to the stability of the interaction between the MCC and the APC/C, perhaps through recruiting APC10 [13].

A clue to how APC15 regulates Cdc20-MCC binding and release might be gleaned from studies in *S. cerevisiae*. While not essential for vegetative divisions, deleting Mnd2 increases the binding of the meiotic co-activator Ama1 to the APC/C [43]. APC15 might, therefore, modulate Cdc20-MCC binding to prevent it 'locking' onto the APC/C. Alternatively, APC15 might present MCC-Cdc20 as a substrate to the APC/C or recruit a release factor. APC15 is located in the right position on the APC/C to influence the binding of the MCC because it seems to interact with APC8, which in turn is needed to bind Cdc20-MCC [13].

Lastly, since the function of APC15 in human cells appears to be primarily linked to the SAC and its depletion prevents mitotic slippage, APC15 may be a candidate for chemotherapeutic drugs.

METHODS

Plasmids and cell lines

APC15 was amplified by PCR from a full-length cDNA clone (ORFeome clone 100066673) obtained from the Mammalian Gene Collection I.M.A.G.E. consortium (Geneservice). For bacterial expression APC15 was cloned with an amino-terminal TEV (tobacco etch virus) cleavage site into pet30a (Novagen). Tetracycline-inducible cell lines expressing APC15-IRES2-mRuby, APC15-3xflag or Cyclin B1-L45A-HA were generated using the FLIP-in system and a modified pCDNA5/FRT/TO vector (Invitrogen). $Cdc20^{K485/490R}$ was generated by site directed mutagenesis of $Cdc20^{WT}$ [5]. The parental tetracycline-inducible RPE1 cell line was created by random integration of an FRT site and a Tet repressor (Invitrogen) gene into RPE1 cells. The tetracyclin-inducible HeLa cell line was a kind gift of S. Taylor, University of Manchester. For siRNA-rescue experiments HeLa and RPE1 cell lines were induced with tetracycline (1 μg/ml) for 12 hours (si-Cdc20) or 72 hours (si-APC15) before analysis, respectively. RPE1 Cyclin B1-Venus and Cyclin A2-Venus cell lines were generated by gene-targeting [46] using a modified protocol (Collin et al., manuscript in preparation).

Cell culture and synchronisation

HeLa cells were maintained in Advanced D-MEM supplemented with 10% FCS and penicillin/streptavidin. RPE1 cells were cultured in F12:DMEM (1:1) media supplemented with 10% FCS, sodium bicarbonate, glutamate and penicillin/streptavidin. Synchronisation in different cell cycle phases was always preceded by a standard double thymidine (2.5 mM) block and release protocol. For G2-phase and G1-phase cells were released into D-MEM for 5 or 18 hours, respectively. Prometaphase cells were collected by mitotic shake off 14 hours after release into Dimethylanastron (DMA) (10 μM), or released for a further two hours into MG132 (10 μM) to obtain a metaphase arrest. To block cells in anaphase, non-degradable cyclin $B1^{L45A}$ was induced at the final release from a double thymidine block. Cells were

released for 12 hours into DMA and then released for a further 80 min into fresh D-MEM and collected by mitotic shake-off. Cycling RPE1 cells were treated with DMA (20 μM), reversine (0.5 μM) or ZM447439 (4 μM). For mitotic slippage studies cycling RPE1 cells were arrested in mitosis with taxol (5 μM).

RNA interference

RPE1 and HeLa cells were transfected with Lipofectamin RNAiMAX (Invitrogen) and siRNA oligonucleotides at 50nM for 85 hours prior to analysis by immunoprecipitation or microscopy if not otherwise stated. For APC10-, APC11-, and UbcH10-depletion, cells were transfected twice: 12 hours before the start, and after the first release during a double-thymidine synchronisation protocol. APC6, APC8, APC10 and APC11 were transfected with a 1:1 mixture of oligo 1 and oligo 2. For experiments characterising the function of APC15 oligo 4 was used. Control and p31^{comet} oligonucleotides were purchased from Invitrogen:

GAPDH D-001830-01,

p31^{comet} oligo1 (5′-UUCUUCGGACUUCUCAUACCACUCC-3′),

p31^{comet} oligo2 (5′-CCGCAACUGUGGAGAAGAUUGGUUU-3′).

APC15 oligonucleotides were purchased from Sigma:

APC15 oligo1 (5′CUGAGACUCUGUGGUUUAA-3′),

APC15 oligo2 (5′-GCCAUCAGUCUGCACUUGA-3′),

APC15 oligo3 (5′-CGAGAUGAAUGACUACAAU-3′),

APC15 oligo4 (5′-GUCUGGUCUAAGUUUCUUU-3′),

APC15 oligo6 (5;-GGAUCGACCCUGUGUGGAA-3′).

The remaining oligonucleotides were obtained from Dharmacon:

APC3 (5′-GGAAAUAGCCGAGAGGUAAUU-3′),

Mad2 (5′-GGAAGAGUCGGGACCACAGUU-3′),

Cdc20 (5′-CGGAAGACCUGCCGUUACAUU-3′),

APC11 oligo 1 (5′-UCUGCAGGAUGGCAUUUAAUU-3′),

APC11 oligo 2 (5′-AAGAUUAAGUGCUGGAACGUU-3′),

APC10 oligo 1 (5′-GAGCUCCAUUGGUAAAUUUUU-3′),

APC10 oligo 2 (5′-GAAAUUGGGUCACAAGCUGUU-3′),

APC6 oligo1 (5′-CUAUGGACCUGCAUGGAUAUU-3′),

APC6 oligo 2 (5′-CGAGGUAACAGUUGACAAAUU-3′),

APC8 oligo 1 (5′-GAAAUUAAAUCCUCGGUAUUU-3′),

APC8 oligo 2 (5′-GCAGUUGCCUAUCACAAUAUU-3′).

Europe PMC Funders Author Manuscripts

UbcH10 oligo (5′-GGUAUAAGCUCUCGCUAGATT-3′).

Microscopy

Before imaging, the culture medium was replaced with Leibovitz's L-15 medium (Gibco BRL) supplemented with 10% foetal bovine serum and penicillin/streptomycin. RPE1 and HeLa cells were imaged on a DeltaVision micrososcope (API, USA) or an ImageXpress Micro widefield system (Molecular Devices, USA). Images were captured at 3 minutes intervals and the fluorescence intensities were measured and analysed using ImageJ software as previously described [11]. For presentation noise reduction was applied using the Sigma filter of the ImageJ software. Statistical analysis was performed using Prism4 software (Graphpad Software). The data were visualised on scatter dot blots showing the mean.

Protein expression, antibodies and quantitative immunoblotting

Polyclonal antibodies were generated by Moravian Biotechnology (Brno, Slovakia) against full-length His-TEV-hAPC15 purified from BL21 *E. coli* using standard techniques. Epitope tags were removed by TEV cleavage prior to immunization. Expression and purification of proteins used for *in vitro* ubiquitylation reactions were performed as previously described [22]. The following antibodies were used at the indicated dilution: APC15 (polyclonal antibody raised full-length APC15, 1:500), Cdc20 (sc-13162, 1:250; Santa Cruz Biotechnology), Cdc20 (sc5296, for immunoprecipitations only; Santa Cruz Biotechnology,), Mad2 (Clone AS55-A12, 1:500; a kind gift of Andrea Musacchio, IFOM, Milan), Mad2 (A300-301A; 1:1000, Bethyl Laboratories), $p31^{comet}$ (Clone E29.19.14, 1:200; a kind gift of Andrea Musacchio), BubR1 (A300-386A, 1:1000; Bethyl Laboratories), Bub3 (611730, 1:500; BD Transduction Laboratories), Cyclin B1 (mAb GNS-1, 1:2000; BD Pharmingen), Cyclin A2 (monoclonal antibody raised against a N-terminal peptide, 1:1000), phospho-H3 S10 (14955, 1:1000; Abcam), α-actin (AC-40, 1:1000, Sigma), APC3 (610455, 1:500; BD Transduction Laboratories), APC3 (clone AF3.1, a kind gift of Tim Hunt, CRUK, London), APC4 (monoclonal antibody raised against a C-terminal peptide, 1:1000), APC11 (monoclonal antibody raised against a C-terminal peptide, 1:500). APC7 (4171, 1:500; Abcam), Cdc16 (sc-6395;, Santa Cruz Biotechnology, 1:500), APC10 (1:2000; raised against full length protein), APC11 (monoclonal antibody raised against a C-terminal peptide, 1:500), UbcH10 (A-650, Boston Biochem, 1:500). Secondary antibodies: Alexa Flour 680 rabbit anti-goat (A21088, Invitrogen), IRDye680 donkey anti-mouse (926-322227, LI-COR), Alexa Fluor 680 goat anti- rabbit (A21076, Invitrogen), IRDye800CW donkey anti-mouse (926-32212, LI-COR), IRDye800CW donkey anti-rabbit (926-32213, LI-COR), anti-mouse IgG-peroxidase (A9044, Sigma) were all used at 1:10000. Quantitative immunoblotting was performed on a LI-COR Odyssey CCD scanner according to the manufacturer's instructions (LI-COR Biosciences).

Immunoprecipitation and size exclusion chromatography

Cells were lysed for 25 minutes on ice in extraction buffer A (50 mM Tris-HCl pH=8.0, 150 mM NaCl, 0.5 % NP-40, 1 mM dithiothreitol (DTT), Roche complete inhibitor cocktail tablet, 0.2 μM microcystin, 1 mM PMSF) and lysates cleared by centrifugation (15 min, 16.100g). Protein complexes were precipitated with antibodies covalently coupled to Dynabeads (Invitrogen), washed in extraction buffer and bound proteins eluted by LDS-sample buffer (Invitrogen). Size-exclusion chromatography was performed on a Superose 6 PC 3.2/30 column (GE Healthcare) as previously described [5] using cells resuspendend in buffer B (175 mM NaCl, 30 mM Hepes pH 7.8, 2.5 mM $MgCl_2$, 10% glycerol, 1 mM dithiothreitol (DTT), 0.2 μM microcystin, 1 mM PMSF).

Europe PMC Funders Author Manuscripts

In vitro ubiquitylation assays and *in vitro* dissociation of checkpoint proteins

In vitro ubiquitylation assays were performed as described previously [22] using APC/C immobilised on APC4 or APC3 beads. Ubiquitylation reactions contained ubiquitin-activating enzyme E1, UbcH10, Ube2S, Cdc20, ubiquitin, ATP, ATP regenerating system, and radio-labelled cyclin B1 (1-86) as a substrate in QPIP buffer (50 mM PIPES at pH 7.5, 100 mM NaCl, 2 mM $MgCl_2$, 10% glycerol, 1 mM DTT and 1 mM EGTA). Mock reactions were performed in QPIP buffer containing 1 μg/ul BSA. Dissociation experiments were performed without (Supplementary Fig. S6c online, mock reactions) or with unlabelled substrate (Fig. 5c).

Statistics

Statistical analyses were performed using GraphPad Prism. Significance of data derived from single cell destruction assays was determined using unpaired, two-tailed Mann-Whitney tests. Binding to APC/C or Cdc20 immunoprecipitates was analysed by paired, two-tailed Student's *t* tests. The results are summarised in Supplementary Information, Table 1 online.

Supplementary Material

Refer to Web version on PubMed Central for supplementary material.

Acknowledgments

We thank S. Taylor for the HeLa FRT cell line, A. Musacchio for the anti-Mad2 and anti-p31^{comet} antibodies and for communicating results before publication, T. Hunt for the anti-APC3 antibody, members of our laboratory for fruitful discussions and O. Nashchekina, F. Walton, E. Russe and S. Wieser for help with somatic cell knock-ins, mass spectrometry, statistical- and flow cytometry analyses, respectively. JM was supported by FEBS and EMBO fellowships. This work was supported by a project grant from the BBSRC and by a Programme grant from Cancer Research UK to JP and core grant support to the Sanger Institute (MOC and JSC) from The Wellcome Trust (grant number 079643/Z/06/Z).

References

1. Sudakin V, Chan GK, Yen TJ. Checkpoint inhibition of the APC/C in HeLa cells is mediated by a complex of BUBR1, BUB3, CDC20, and MAD2. The Journal of cell biology. 2001; 154:925–936. [PubMed: 11535616]
2. Zeng X, et al. Pharmacologic inhibition of the anaphase-promoting complex induces a spindle checkpoint-dependent mitotic arrest in the absence of spindle damage. Cancer cell. 2010; 18:382–395. [PubMed: 20951947]
3. Visconti R, Palazzo L, Grieco D. Requirement for proteolysis in spindle assembly checkpoint silencing. Cell cycle (Georgetown, Tex. 2010; 9:564–569.
4. Reddy SK, Rape M, Margansky WA, Kirschner MW. Ubiquitination by the anaphase-promoting complex drives spindle checkpoint inactivation. Nature. 2007; 446:921–925. [PubMed: 17443186]
5. Nilsson J, Yekezare M, Minshull J, Pines J. The APC/C maintains the spindle assembly checkpoint by targeting Cdc20 for destruction. Nature cell biology. 2008; 10:1411–1420.
6. Yoon HJ, et al. Proteomics analysis identifies new components of the fission and budding yeast anaphase-promoting complexes. Curr Biol. 2002; 12:2048–2054. [PubMed: 12477395]
7. Hall MC, Torres MP, Schroeder GK, Borchers CH. Mnd2 and Swm1 are core subunits of the Saccharomyces cerevisiae anaphase-promoting complex. The Journal of biological chemistry. 2003; 278:16698–16705. [PubMed: 12609981]
8. Schreiber A, et al. Structural basis for the subunit assembly of the anaphase-promoting complex. Nature. 2011; 470:227–232. [PubMed: 21307936]
9. Penkner AM, Prinz S, Ferscha S, Klein F. Mnd2, an essential antagonist of the anaphase-promoting complex during meiotic prophase. Cell. 2005; 120:789–801. [PubMed: 15797380]

10. Hubner NC, et al. Quantitative proteomics combined with BAC TransgeneOmics reveals in vivo protein interactions. The Journal of cell biology. 2010; 189:739–754. [PubMed: 20479470]
11. Clute P, Pines J. Temporal and spatial control of cyclin B1 destruction in metaphase. Nature cell biology. 1999; 1:82–87.
12. Thornton BR, et al. An architectural map of the anaphase-promoting complex. Genes & development. 2006; 20:449–460. [PubMed: 16481473]
13. Izawa D, Pines J. How APC/C-Cdc20 changes its substrate specificity in mitosis. Nature cell biology. 2011; 13:223–233.
14. Di Fiore B, Pines J. How cyclin A destruction escapes the spindle assembly checkpoint. The Journal of cell biology. 2010; 190:501–509. [PubMed: 20733051]
15. Ge S, Skaar JR, Pagano M. APC/C- and Mad2-mediated degradation of Cdc20 during spindle checkpoint activation. Cell cycle (Georgetown, Tex. 2009; 8:167–171.
16. Pan J, Chen RH. Spindle checkpoint regulates Cdc20p stability in Saccharomyces cerevisiae. Genes & development. 2004; 18:1439–1451. [PubMed: 15198982]
17. Kulukian A, Han JS, Cleveland DW. Unattached kinetochores catalyze production of an anaphase inhibitor that requires a Mad2 template to prime Cdc20 for BubR1 binding. Developmental cell. 2009; 16:105–117. [PubMed: 19154722]
18. Meraldi P, Draviam VM, Sorger PK. Timing and checkpoints in the regulation of mitotic progression. Developmental cell. 2004; 7:45–60. [PubMed: 15239953]
19. Dobles M, Liberal V, Scott ML, Benezra R, Sorger PK. Chromosome missegregation and apoptosis in mice lacking the mitotic checkpoint protein Mad2. Cell. 2000; 101:635–645. [PubMed: 10892650]
20. Santaguida S, Tighe A, D'Alise AM, Taylor SS, Musacchio A. Dissecting the role of MPS1 in chromosome biorientation and the spindle checkpoint through the small molecule inhibitor reversine. The Journal of cell biology. 2010; 190:73–87. [PubMed: 20624901]
21. Carroll CW, Morgan DO. The Doc1 subunit is a processivity factor for the anaphase-promoting complex. Nature cell biology. 2002; 4:880–887.
22. Garnett MJ, et al. UBE2S elongates ubiquitin chains on APC/C substrates to promote mitotic exit. Nature cell biology. 2009; 11:1363–1369.
23. Yang M, et al. p31(comet) Blocks Mad2 Activation through Structural Mimicry. Cell. 2007; 131:744–755. [PubMed: 18022368]
24. Xia G, et al. Conformation-specific binding of p31(comet) antagonizes the function of Mad2 in the spindle checkpoint. The EMBO journal. 2004; 23:3133–3143. [PubMed: 15257285]
25. Mapelli M, et al. Determinants of conformational dimerization of Mad2 and its inhibition by p31comet. The EMBO journal. 2006; 25:1273–1284. [PubMed: 16525508]
26. Habu T, Kim SH, Weinstein J, Matsumoto T. Identification of a MAD2-binding protein, CMT2, and its role in mitosis. The EMBO journal. 2002; 21:6419–6428. [PubMed: 12456649]
27. Varetti, G.; Guida, C.; Santaguida, S.; Chiroli, E.; Musacchio, A. p31Comet-stimulated degradation of Cdc20 is required for timely mitotic exit and spindle checkpoint adaptation. 2011. submitted
28. Herzog F, et al. Structure of the Anaphase-Promoting Complex/Cyclosome Interacting with a Mitotic Checkpoint Complex. Science (New York, N.Y. 2009; 323:1477–1481.
29. Gascoigne KE, Taylor SS. Cancer cells display profound intra- and interline variation following prolonged exposure to antimitotic drugs. Cancer cell. 2008; 14:111–122. [PubMed: 18656424]
30. Huang HC, Shi J, Orth JD, Mitchison TJ. Evidence that mitotic exit is a better cancer therapeutic target than spindle assembly. Cancer cell. 2009; 16:347–358. [PubMed: 19800579]
31. Brito DA, Rieder CL. Mitotic checkpoint slippage in humans occurs via cyclin B destruction in the presence of an active checkpoint. Curr Biol. 2006; 16:1194–1200. [PubMed: 16782009]
32. Nezi L, Musacchio A. Sister chromatid tension and the spindle assembly checkpoint. Curr Opin Cell Biol. 2009; 21:785–795. [PubMed: 19846287]
33. Ditchfield C, et al. Aurora B couples chromosome alignment with anaphase by targeting BubR1, Mad2, and Cenp-E to kinetochores. The Journal of cell biology. 2003; 161:267–280. [PubMed: 12719470]

34. Miniowitz-Shemtov S, Teichner A, Sitry-Shevah D, Hershko A. ATP is required for the release of the anaphase-promoting complex/cyclosome from inhibition by the mitotic checkpoint. Proceedings of the National Academy of Sciences of the United States of America. 2010; 107:5351–5356. [PubMed: 20212161]
35. Ma HT, Poon RY. Orderly inactivation of the key checkpoint protein mitotic arrest deficient 2 (MAD2) during mitotic progression. The Journal of biological chemistry. 2011
36. Danielsen JM, et al. Mass spectrometric analysis of lysine ubiquitylation reveals promiscuity at site level. Molecular & cellular proteomics : MCP. 2011; 10:M110. 003590.
37. Gmachl M, Gieffers C, Podtelejnikov AV, Mann M, Peters JM. The RING-H2 finger protein APC11 and the E2 enzyme UBC4 are sufficient to ubiquitinate substrates of the anaphase-promoting complex. Proceedings of the National Academy of Sciences of the United States of America. 2000; 97:8973–8978. [PubMed: 10922056]
38. Leverson JD, et al. The APC11 RING-H2 finger mediates E2-dependent ubiquitination. Molecular biology of the cell. 2000; 11:2315–2325. [PubMed: 10888670]
39. Williamson A, et al. Identification of a physiological E2 module for the human anaphase-promoting complex. Proceedings of the National Academy of Sciences. 2009
40. Walker A, Acquaviva C, Matsusaka T, Koop L, Pines J. UbcH10 has a rate-limiting role in G1 phase but might not act in the spindle checkpoint or as part of an autonomous oscillator. Journal of cell science. 2008; 121:2319–2326. [PubMed: 18559889]
41. Stegmeier F, et al. Anaphase initiation is regulated by antagonistic ubiquitination and deubiquitination activities. Nature. 2007; 446:876–881. [PubMed: 17443180]
42. Choi E, et al. BubR1 acetylation at prometaphase is required for modulating APC/C activity and timing of mitosis. The EMBO journal. 2009; 28:2077–2089. [PubMed: 19407811]
43. Oelschlaegel T, et al. The yeast APC/C subunit Mnd2 prevents premature sister chromatid separation triggered by the meiosis-specific APC/C-Ama1. Cell. 2005; 120:773–788. [PubMed: 15797379]
44. Maciejowski J, et al. Mps1 directs the assembly of Cdc20 inhibitory complexes during interphase and mitosis to control M phase timing and spindle checkpoint signaling. The Journal of cell biology. 2010; 190:89–100. [PubMed: 20624902]
45. De Antoni A, et al. The Mad1/Mad2 complex as a template for Mad2 activation in the spindle assembly checkpoint. Curr Biol. 2005; 15:214–225. [PubMed: 15694304]
46. Berdougo E, Terret ME, Jallepalli PV. Functional dissection of mitotic regulators through gene targeting in human somatic cells. Methods Mol Biol. 2009; 545:21–37. [PubMed: 19475380]

Europe PMC Funders Author Manuscripts

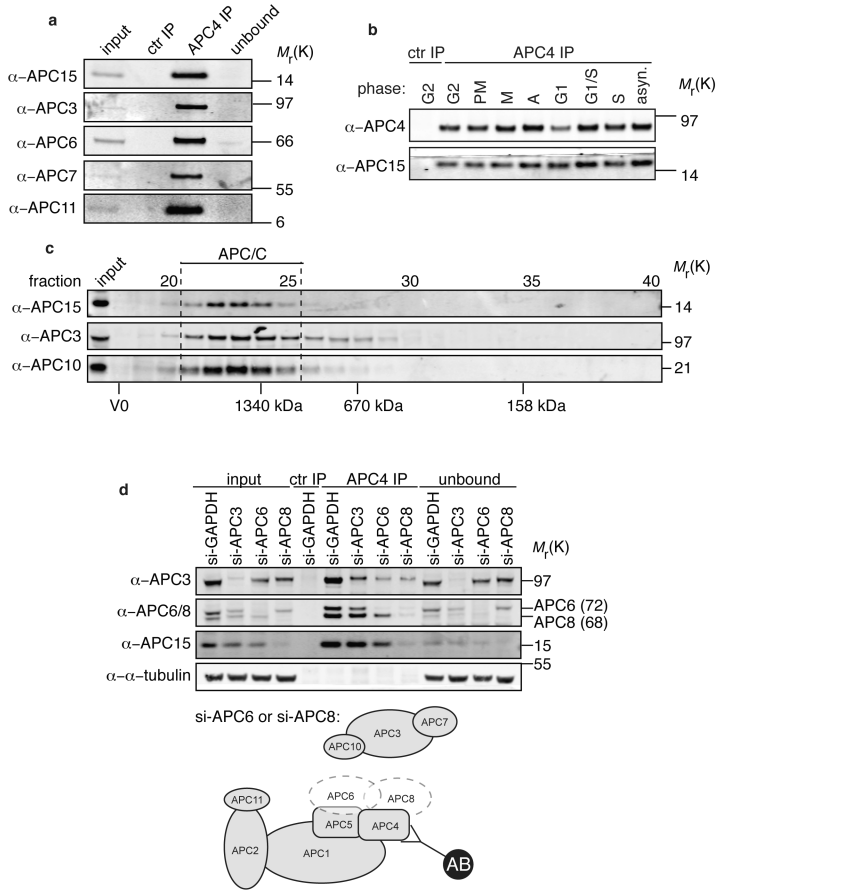

Figure 1.

APC15 is a subunit of the human APC/C. (**a**) APC4 was immunoprecipitated from asynchronously growing HeLa cells and the co-precipitating APC/C subunits were analysed by immunoblotting with the indicated antibodies. (**b**) HeLa cells were synchronised at different stages of the cell cycle and analysed as in (a). (**c**) Typical size-exclusion chromatography of an extract from prometaphase-arrested HeLa cells. The fractions were analysed by immunoblot (V_0=void volume) with the indicated antibodies. (**d**) Anti-APC4 immunoprecipitations using extracts from prometaphase-arrested HeLa cells that were treated with 50 nM of the indicated siRNAs for 72h. Note, that depleting APC6 or APC8 causes the APC/C to dissociate into two subcomplexes [13], one of which was precipitated with anti-APC4 and the other with anti-APC3 (see cartoon and Supplementary Fig. S2b online). Molecular mass markers on the right of each panel. Results in each panel representative of at least three experiments.

Europe PMC Funders Author Manuscripts

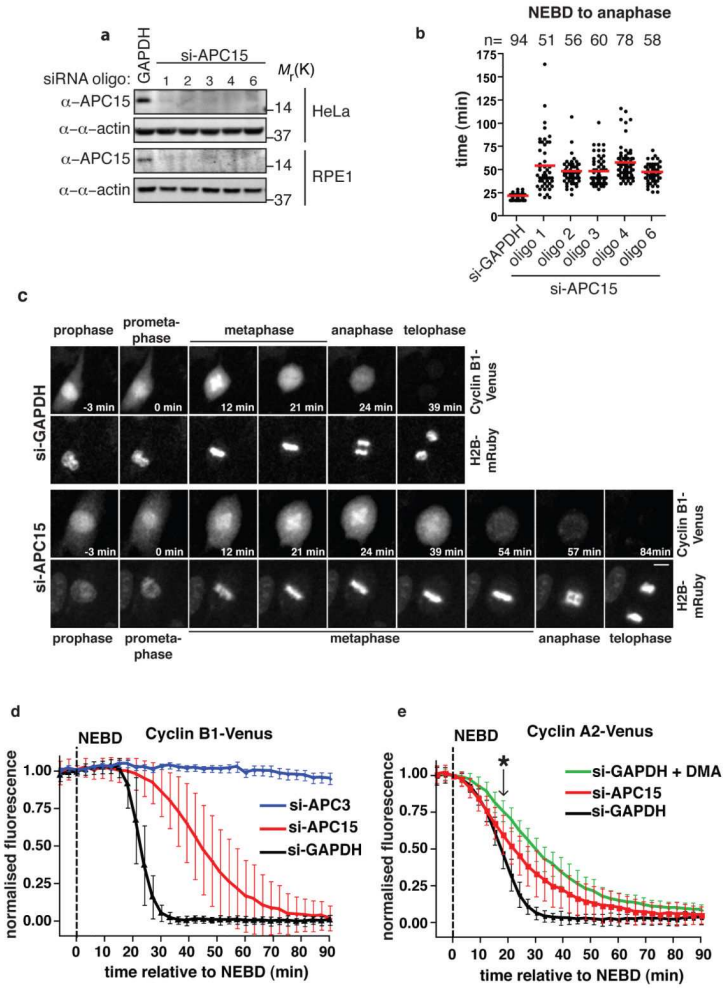

Figure 2.

APC15 is an APC/C subunit required for timely entry into anaphase. (**a**) HeLa (top) or RPE1 (bottom) cells were treated for 85h with 50 nM of the indicated siRNAs before analysis by immunoblot. Molecular mass markers on the right. Results representative of three experiments. (**b**) The time from NEBD to anaphase of asynchronously growing RPE1-Cyclin B1-Venus cells, treated as in (**a**), was determined by fluorescence and phase-contrast microscopy. Scatter dot blots show the mean (red line) of the indicated number of cells from three experiments ($p<0.0001$ versus si-GAPDH for each oligo, Supplementary Table 1). (**c**) Montage of representative images showing RPE1-Cyclin B1-Venus/H2B-mRuby expressing cells treated as in (**a**) using APC15 oligo 4. NEBD set to 0 min. Scale bar, 10 μm. (**d** and **e**) Single-cell destruction assays of asynchronously growing RPE1-Cyclin B1-Venus (**d**) and RPE1-Cyclin A2-Venus (**e**) cells after 85h siRNA-treatment. Images were captured every three minutes and the total cell fluorescence was measured. Fluorescence intensities were normalised to NEBD. Error bars indicate s.d. from 25 cells for si-GAPDH and si-APC15 and 15 cells for si-APC3 from three experiments. Only cells that arrested for more than 100 minutes were quantified in si-APC3 experiments. The asterisk (*) indicates the time-point before the beginning of anaphase in si-GAPDH-treated cells.

Europe PMC Funders Author Manuscripts

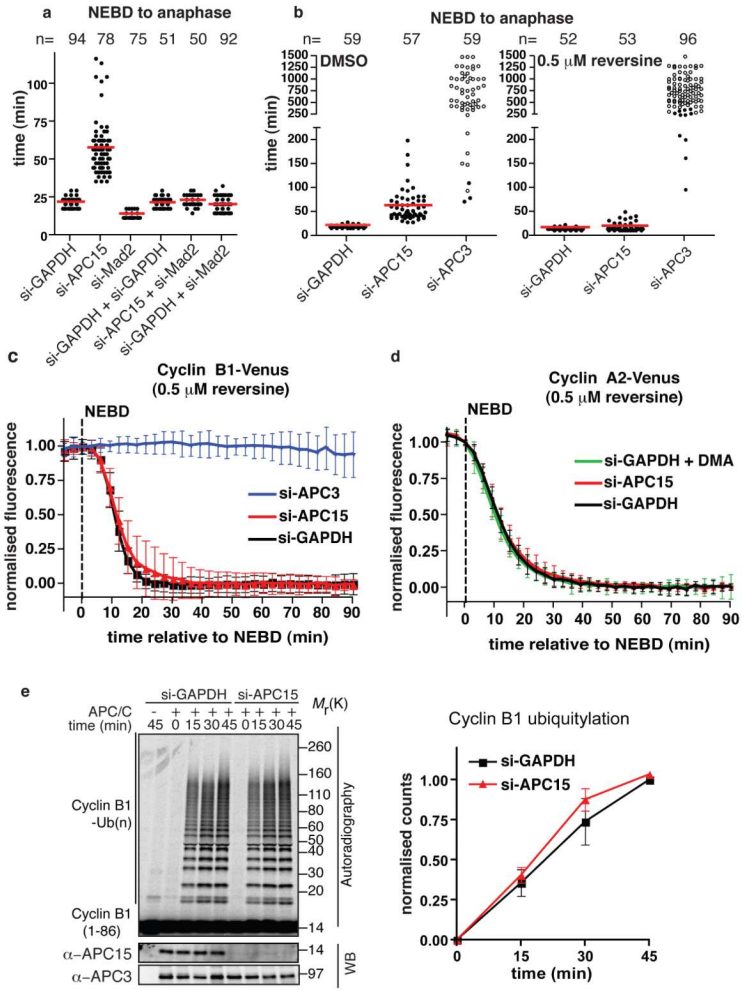

Figure 3.

APC15 depletion causes a SAC-dependent delay in mitosis but does not affect APC/C activity. (**a** and **b**) The timing from NEBD to anaphase of asynchronously growing RPE1-Cyclin B1-Venus cells treated for 85h with the indicated siRNAs was determined by microscopy. Si-GAPDH and si-APC15 are identical to Fig. 2b as the data are derived from the same experiments. DMSO or 0.5 μM reversine was added as indicated. Scatter dot blots show the mean (red line) of the indicated number of cells from three experiments ($p<0.0001$ for si-APC15 versus si-GAPDH in (a) and (b, DMSO panel), Supplementary Table 1 online). Open circles indicate the minimal time that cells were arrested when NEBD or anaphase was not observed during the experiment. (**c** and **d**) Cells were treated as in Fig 2d, e but with 0.5 μM reversine added to the medium before imaging. Error bars indicate s.d. from 50 cells for si-GAPDH and si-APC15, ten cells for si-APC3 from three experiments (**c**) or 25 cells for si-GAPDH and si-APC15, and 50 cells for si-GAPDH + DMA from two experiments, respectively (**d**). (**e**) Autoradiography of an *in vitro* ubiquitylation assay using interphase APC/C purified from GAPDH- and APC15-depleted cells. The APC/C was immunoprecipitated using anti-APC3 antibodies, activated with Cdh1, and probed for its ability to ubiquitylate Cyclin B1 (aa 1-86). Molecular mass markers on the right. The quantification shows Cyclin B1 ubiquitylation normalised to si-GAPDH APC/C (mean ± s.e.m from three experiments).

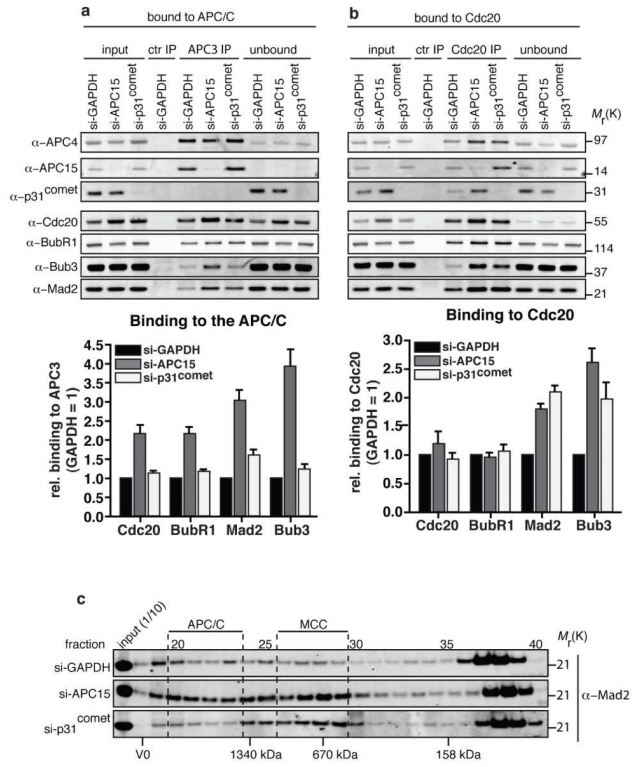

Figure 4.

APC15 is required for the turnover of Mad2, BubR1, Bub3 and Cdc20 on the APC/C during prometaphase**.** (**a** and **b**) Anti-APC3 (a) and anti-Cdc20 (b) immunoprecipitates from HeLa cells arrested in prometaphase and treated with the indicated siRNAs for 85h, were analysed by immunoblotting.

The amounts of MCC proteins that precipitated with APC3 or Cdc20 were analysed by quantitative immuno-blotting and normalised to si-GAPDH-treatment. Molecular mass markers on right. Bar charts indicate the mean ± s.e.m. from six experiments. **(c)** Anti-Mad2 immunoblots of fractions from size exclusion chromatography analyses of HeLa cell extracts treated as in (**a**). Molecular mass markers on the right. The complete immunoblot analyses are shown in the Supplementary Information Fig. S5a-c online. Results representative of two experiments.

Europe PMC Funders Author Manuscripts

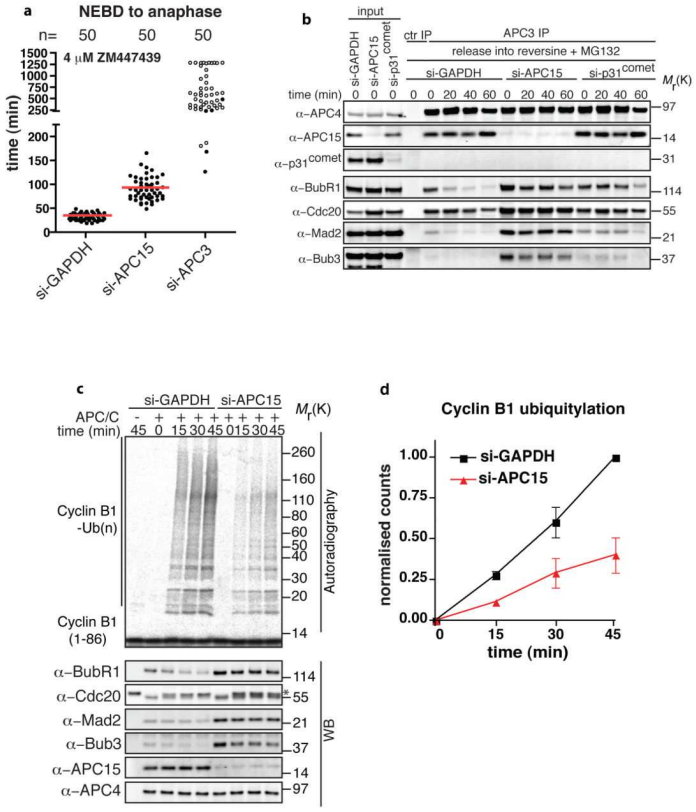

Figure 5.

APC15 is required for the release of Mad2, BubR1 and Bub3 from the APC/C after the SAC had been satisfied. (**a**) Timing from NEBD to anaphase in the presence of 4 μM ZM447439 in RPE1-Cyclin B1-Venus cells treated as in Fig 3b. Scatter dot blots show the mean (red line) of the indicated number of cells from three experiments ($p<0.0001$ for si-APC15 versus si-GAPDH, Supplementary Table 1 online). Open circles indicate the minimal time that cells were arrested when NEBD or anaphase was not observed during the experiment. We noted that adding 4 μM ZM447439 slowed progress from NEBD to anaphase by a factor of ~1.5 independently of siRNA treatment (compare Fig. 5a and Fig. 3a). A similar delay has been previously reported in RPE-1 cells [44] and might reflect the extended time ZM447439-treated cells spend in prometaphase [33]. (**b**) HeLa cells were released from a DMA-block into fresh medium containing 0.5 μM reversine and 10 μM MG132. Samples were collected at the indicated time-points and the APC/C immunoprecipitated using anti-APC3 antibodies before analysis by immunoblotting with the indicated antibodies. Molecular mass markers on the right. The quantification of three experiments is shown in Supplementary Fig. S6b online). (**c**) Autoradiography of *in vitro* ubiquitylation assays using APC/C purified from si-GAPDH- and si-APC15-treated HeLa cells arrested in prometaphase. The amounts of SAC proteins bound to the APC/C were determined by immunoblotting an *in vitro* ubiquitylation assay done in parallel. The asterisk (*) denotes His-Cdc20 that binds to the APC/C, the lower band is endogenous Cdc20. Molecular mass markers on the right. The quantification of two experiments is shown in Supplementary Fig. S6e online. **(d)** Quantification of ubiquitylated Cyclin B1 (1-86) normalised to control reactions from three experiments (mean ± s.e.m).

Europe PMC Funders Author Manuscripts

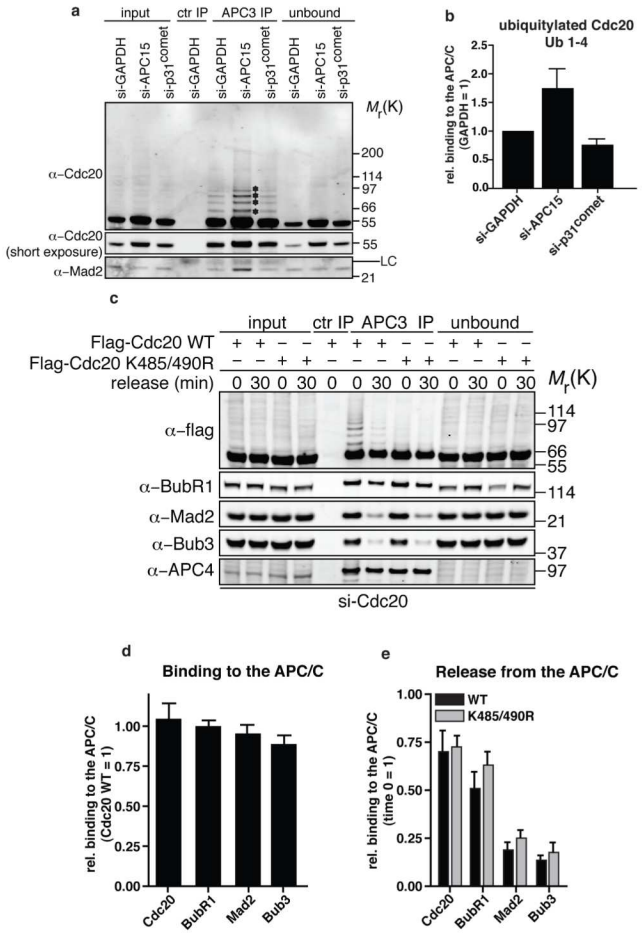

Figure 6.

Ubiquitylation of Cdc20 is not required to release MCCs from the APC/C. (**a**) Immuno-blot analysis of Cdc20 ubiquitylation from the experiments shown in Fig 4a. LC denotes the light chain of Cdc20 antibodies. Molecular mass markers on the right. (**b**) Ubiquitylated Cdc20 was analysed by quantitative Western blotting from four experiments shown in Fig. 4a. To determine the relative amount of ubiquitylated Cdc20 on the APC/C the ratio of Cdc20 modified with one to four ubiquitin molecules (Ub1-4, indicated by asterisks) in si-GAPDH- versus si-APC15- or si-p31^{comet} treatment was determined and normalised to the ratio of unmodified Cdc20. The value for si-GAPDH-treated cells was set to 1. Bar charts indicate the mean ± s.e.m. of four experiments (**c**). Stable cell lines expressing siRNA-resistant Flag-Cdc20^{WT} or Flag-Cdc20$^{K485/490R}$ from an inducible promoter were treated with si-Cdc20 oligonucleotides for 72h. The cells were arrested with DMA, and then released into fresh medium containing 0.5 μM reversine and 10 μM MG132. Samples were collected at the indicated time-points and the APC/C immunoprecipitated using anti-APC3 antibodies before immunoblot analysis with the indicated antibodies. Molecular mass markers on the right. (**d**) The amount of MCC components bound to the APC/C during the DMA arrest (t=0) was determined for Cdc20$^{K485/490R}$ and normalised to Cdc20^{WT}. (**e**) The amount of MCC components bound to the APC/C 30 minutes after release from the DMA block was normalised to time-point zero (t=0). Bar charts indicate the mean ± s.e.m. of three experiments for (d) and (e).

Europe PMC Funders Author Manuscripts

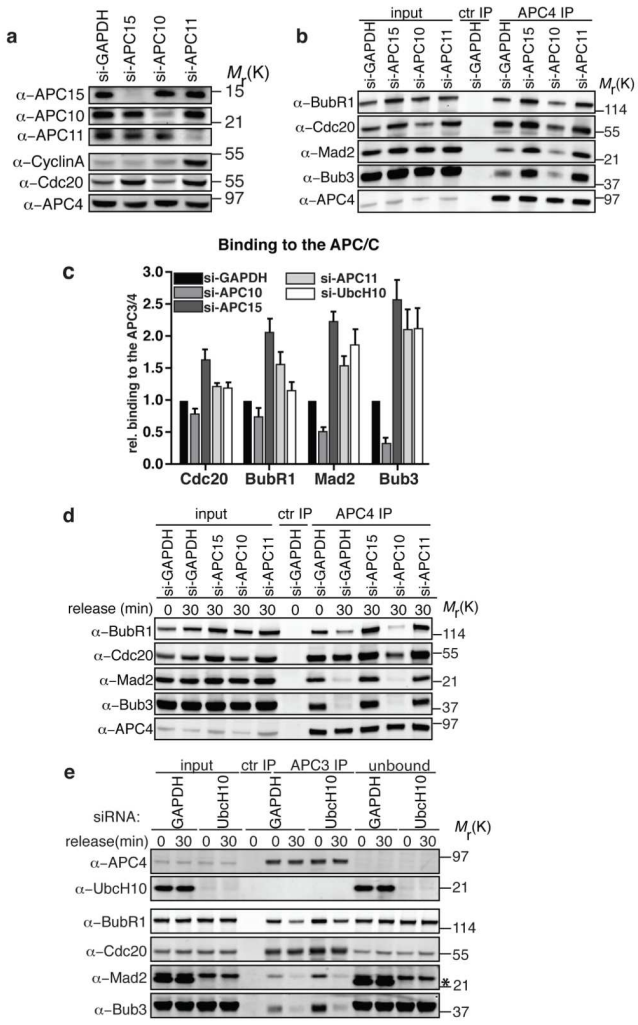

Figure 7.

Ubiquitylation contributes to the release of MCCs from the APC/C. (**a**) Immunoblot analysis with the indicated antibodies of total cell extracts from DMA-arrested HeLa cells that were treated with the indicated siRNAs using a double transfection protocol (see Supplementary Methods online). Molecular mass markers on the right. (**b**) Immunoblot analysis of anti-APC4 immunoprecipitates from cell extracts shown in (**a**) with the indicated antibodies. (**c**) Quantification of the amount of APC/C-bound SAC proteins during a DMA-arrest shown in (b) and (e, t=0) relative to si-GAPDH-treated APC/C. Bar charts indicate the mean ± s.e.m. of six experiments for (b) and of four experiments for (e). (**d**) HeLa cells from (b) were released for 30 min into fresh medium containing 0.5 μM reversine and 10 μM MG132 and the APC/C precipitated by APC4 antibodies before immunoblot analysis with the indicated antibodies. (**e**) HeLa cells treated with the indicated siRNAs were arrested as in (a, t=0) and released as in (d, t=30). Anti-APC3 immunoprecipitates from the indicated time points were analysed with the indicated antibodies. The quantification of MCC binding before the release is shown in (c). The asterisk denotes the UbcH10 signal derived from the first immune-detection. Molecular mass markers on the right.

Europe PMC Funders Author Manuscripts